DOI 10.5012/bkcs.2011.32.1.141

Low-temperature Synthesis of Highly Crystalline $Ba_xSr_{1-x}TiO_3$ Nanoparticles in Aqueous Medium

Yong Joo Kim, Sher Bahadur Rawal, Sang Do Sung, and Wan In Lee*

*Department of Chemistry, Inha University, Incheon 402-751, Korea. *E-mail: wanin@inha.ac.kr*
Received October 23, 2010, Accepted November 2, 2010

We report the synthesis of $SrTiO_3$, $BaTiO_3$ and $Ba_xSr_{1-x}TiO_3$ (BST) nanoparticles (NPs) in various compositions (x = 0.25, 0.5 and 0.75) by an inorganic sol-gel method under a basic condition. Highly crystalline nanoparticles were formed at the reaction temperature of 25 - 100 °C from a stabilized titanium alkoxide in tetramethylammonium hydroxide (TMAH) and barium or strontium acetate in aqueous solution. Morphology and particle structure of the synthesized BST NPs were characterized by scanning electron microscopy (SEM), X-ray diffraction (XRD) and transmission electron microscopy (TEM). The BST nanoparticles in various compositions were monodispersed without mutual aggregation, and their average sizes were in the range of 70 - 80 nm. Furthermore, they showed highly crystallized perovskite phase over the whole composition range from $SrTiO_3$ to $BaTiO_3$. We also proposed a mechanism for the low-temperature formation of BST NPs.

Key Words: Barium strontium titanate, Nanoparticles, Tetrametylammonium hydroxide, Sol-gel, Low-temperature synthesis

Introduction

ABO_3 perovskite compounds such as $BaTiO_3$ and $SrTiO_3$ have received extensive attention due to their unique electrical properties applicable to various electronic devices.[1-3] The $BaTiO_3$, $SrTiO_3$ or their solid solutions ($Ba_xSr_{1-x}TiO_3$, $x = 0 \sim 1$, BST) demonstrate outstanding dielectric, ferroelectric, pyroelectric and/or piezoelectric properties. It is well-known that these properties critically depend on their chemical compositions and structural characteristics.[3-9] That is, the electrical and electronic properties of $BaTiO_3$, $SrTiO_3$ and $Ba_xSr_{1-x}TiO_3$ (BST) can be modified according to the Ba content in the solid solution, crystallinity, particle size and shape, and others. For instance, their ferroelectric Curie temperatures can be tuned by changing the strontium to barium ratio in $Ba_xSr_{1-x}TiO_3$.[5]

Thus far, many synthetic methods such as solid-state reaction,[10] coprecipitation,[11] hydrothermal reaction[12] and sol-gel method[13,14] have been applied for the preparation of BST nanoparticles. Among them, the solid-state reaction would be the most popular and convenient method in preparing BST powders, but it normally requires the calcination at high temperatures above 1000 °C.[15] Even though the as-obtained BST powders by this reaction are highly crystallized, their microstructures are not homogeneous and the particles are very large in size and heavily aggregated.[5,16] Hydrothermal method, usually performed under an elevated pressure caused by solvent vapor, provides an alternative route in synthesizing $BaTiO_3$, $SrTiO_3$ and $Ba_{1-x}Sr_xTiO_3$ particles at a relatively low temperature.[17-20] However, the exact composition control for these mixed metal oxides is quite difficult, even though the synthesized particles are relatively uniform in size and shape.[20] In tailoring the chemical composition for these mixed metal oxides, sol-gel method is considered to be one of the most suitable techniques.[21,22] The sol-gel method, based on the hydrolysis of metal alkoxides, stabilized by organic stabilizers, and subsequent calcinations to achieve crystallized phase, generally requires the calcination at high temperature and long reaction time. Furthermore, the prepared particles are severely aggregated, and the particle size and shape are not uniform at all.

Previously, Wada *et al*. reported a low-temperature procedure in preparing the $BaTiO_3$ particles by an inorganic sol-gel method in a highly basic condition.[22] In the present work, we modified and generalized the synthetic technique to prepare the $Ba_xSr_{1-x}TiO_3$ nanoparticles with various compositions (x = 0, 0.25, 0.5, 0.75, 1). The highly crystallized BST nanoparticles with the pure perovskite phase were successfully prepared at 25 - 100 °C in a flask, and they were monodispersed and stably dispersed in aqueous solution.

Experimental Section

Synthesis of BST Nanoparticles. Highly crystalline $Ba_xSr_{1-x}TiO_3$ (BST, x = 0, 0.25, 0.5, 0.75, 1) nanoparticles were synthesized by sol-gel reaction in aqueous solution. Titanium tetraisopropoxide (TTIP, 97%, Aldrich Chemical Co.; 2 mmol) was slowly added drop-wise to 20 mL of tetramethylammonium hydroxide (TMAH, 97%, Aldrich Chemical Co.; 4 mmol) aqueous solution under vigorous stirring. At the initial stage of reaction, the white precipitate was formed in the solution. After refluxing at 100 °C for 30 min, the solution turned to clear. Barium acetate (99%, Aldrich Chemical Co.) and strontium acetate (Aldrich Chemical Co.) with variable composition (Ba_xSr_{1-x} to Ti molar ratio is 1.0, where x = 0, 0.25, 0.5, 0.75, 1) were added to the above stabilized Ti-precursor solution under vigorous stirring. The BST nanoparticles were formed by further refluxing at 25 - 100 °C for 6 - 24 hr. The as-prepared BST nanoparticles were washed with water, and dried in vacuum oven.

Characterization. X-ray diffraction (XRD) patterns for the BST nanoparticles were obtained by using a Rigaku Multiflex diffractometer with a monochromated light-intensity Cu Kα radiation at 40 kV and 20 mV settings. For the morphological

characterization of synthesized nanoparticles by a field emission scanning electron microscope (FE-SEM, Hitachi S-4200) and TEM (Philips CM30 transmission electron microscope operated at 200 kV), 1 mg of BST sample were dispersed in 50 mL of ethanol and a drop of the suspension was then spread on a holey amorphous carbon coated Ni grid (JEOL Ltd.).

Results and Discussion

$SrTiO_3$ and $BaTiO_3$ nanoparticles were synthesized by an inorganic sol-gel reaction under a basic environment. These nanoparticles were formed at low temperature from a mixture of titanium alkoxide stabilized by TMAH and strontium (or barium) acetate dissolved in aqueous solution. As shown in the XRD patterns of Figure 1a, the $SrTiO_3$ nanoparticles synthesized at several reaction temperatures are in the pure perovskite phase. Even at room temperature, the synthesized $SrTiO_3$ particles were highly crystallized without formation of other impurity phases. The increase of peak intensity and decrease of line width suggest that the crystallinity of $SrTiO_3$ gradually increased with elevation of reaction temperature. The crystallite sizes calculated from the (110) peak by applying Scherrer equation were 34 nm for the particles prepared at 25 °C, 38 nm at 50 °C, and 51 nm at 100 °C, which clearly indicates that the highly crystallized $SrTiO_3$ can be obtained at very low reaction temperatures. The $SrTiO_3$ nanoparticles prepared at 100 °C were analyzed by TEM, as shown in Figure 2a-c. Low magnification images in Figure 2a and 2b indicate that the prepared $SrTiO_3$ nanoparticles are a spherical shape with an average diameter of 80 nm, and they are highly monodispersed and mutually separated without agglomeration. Figure 2c shows the high resolution TEM image obtained from a part of the $SrTiO_3$ nanoparticle in Figure 2b. Uniform fringes with an interval of 0.390 nm, corresponding to the (100) lattice spacing of the perovskite phase, were observed over the entire particle. This suggests that each nanoparticle consists of a single perovskite grain.

Figure 1b shows the XRD patterns of the $BaTiO_3$ nanoparticles prepared at several different reaction temperatures. It was observed that the $BaTiO_3$ particles prepared at room temperature were amorphous. At the reaction temperatures of 50 °C, however, the $BaTiO_3$ particles began to be crystallized and their crystallinity was further improved as elevating the reaction temperature to 100 °C. Figure 2d shows TEM image for the $BaTiO_3$ nanoparticles prepared at 100 °C. The nanoparticles were also a spherical structure, but their diameter (~70 nm) seemed to be slightly smaller than that of $SrTiO_3$.

The BST ($Ba_xSr_{1-x}TiO_3$) nanoparticles, solid solutions between $SrTiO_3$ and $BaTiO_3$ with the compositions of $x = 0$, 0.25, 0.5, 0.75 and 1.0 were then prepared by the above mentioned inorganic sol-gel method at 100 °C. As shown in the XRD patterns of Figure 3a, the synthesized BST particles present the highly crystallized perovskite phase, regardless of relative composition between Sr and Ba. This clearly indicates that the complete solid solution can be formed over the whole composition range. Figure 3b shows the wide-angle-view of the (110) XRD peaks for the prepared BST nanoparticles in various Ba/Sr molar ratios. It was seen that the positions of (110) peaks were shifted to lower angle with increasing the Ba mol fraction, which is indicative that the lattice parameter of BST is gradually

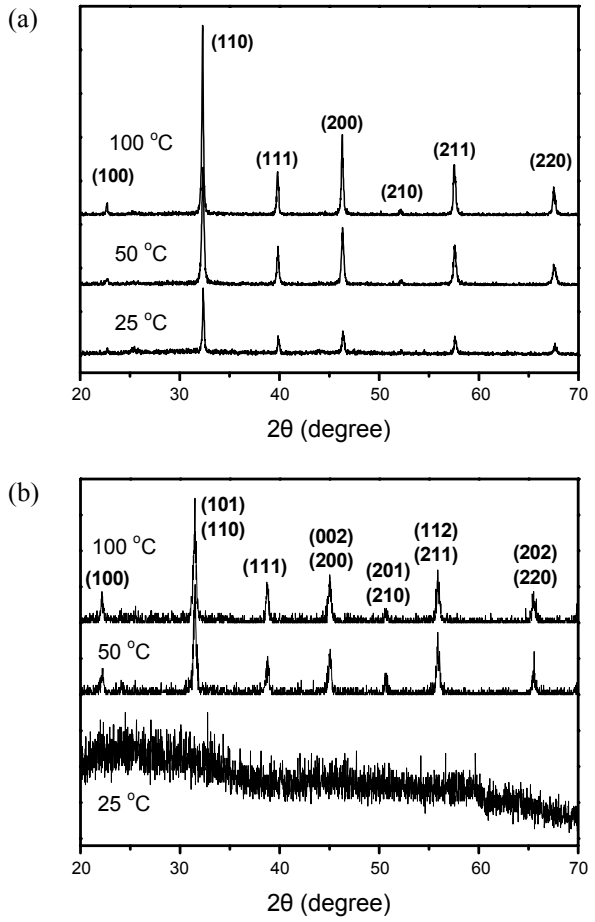

Figure 1. XRD patterns of the as-prepared $SrTiO_3$ (a) and $BaTiO_3$ (b) nanoparticles at several reaction temperatures.

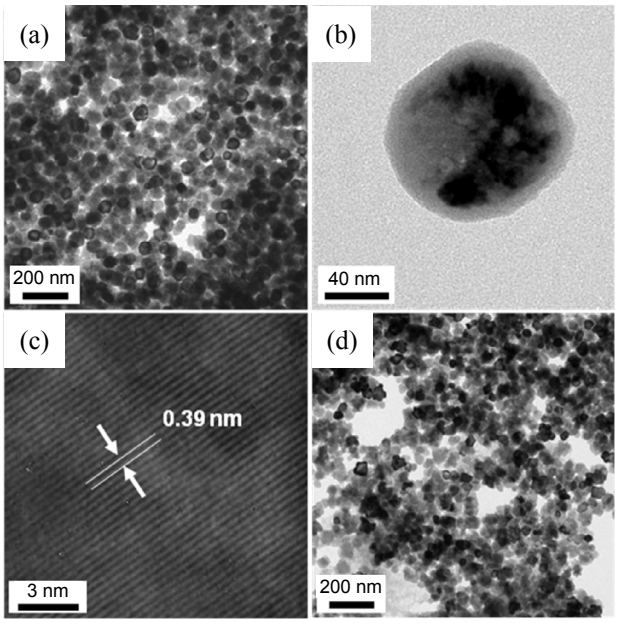

Figure 2. TEM images of the $SrTiO_3$ nanoparticles (a-c) and the $BaTiO_3$ nanoparticles (d).

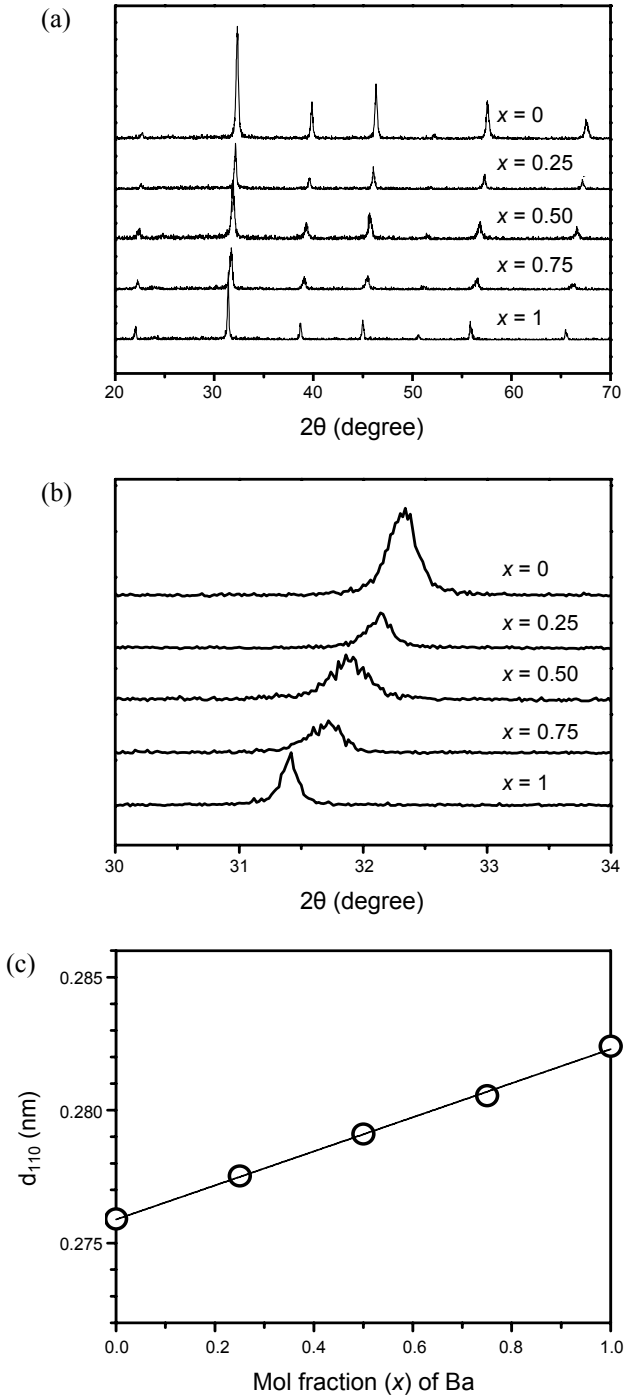

Figure 3. XRD patterns of the as-prepared $Ba_xSr_{1-x}TiO_3$ (BST) nanoparticles with different Ba mol fractions (a), and their wide-angle XRD patterns for the (110) peaks (b). Plot (c) describes the change of d_{110} as a function of Ba mol fraction in BST nanoparticles. For all cases, the synthetic reactions were carried out at 100 ^oC for 6 hr.

increased, as the content of Ba^{2+} ion, which is bigger than Sr^{2+}, is increased from 0 to 100%. Figure 3c plots the change of BST cell parameter as a function of Ba composition. A linear increase of the cell parameter suggests that the complete solid solutions between $SrTiO_3$ and $BaTiO_3$ have been formed in the synthesized BST nanoparticles, according to the Vegard's law.

SEM images in Figure 4a-c show the as-prepared BST nanoparticles in the compositions of $x = 0.25$, 0.50 and 0.75, respectively. For the all BST samples, individual particles are monodispersed and their average diameters were slightly decreased, as the Ba content increased. That is, the average size of $Ba_{0.25}Sr_{0.75}TiO_3$ was close to 80 nm, whereas that of $Ba_{0.75}Sr_{0.25}TiO_3$ was close to 70 nm. TEM image in Figure 4d showed the as-prepared $Ba_{0.5}Sr_{0.5}TiO_3$ nanoparticles. The individual nanoparticles were reasonably monodispersed and seem to be mutually separated without aggregation.

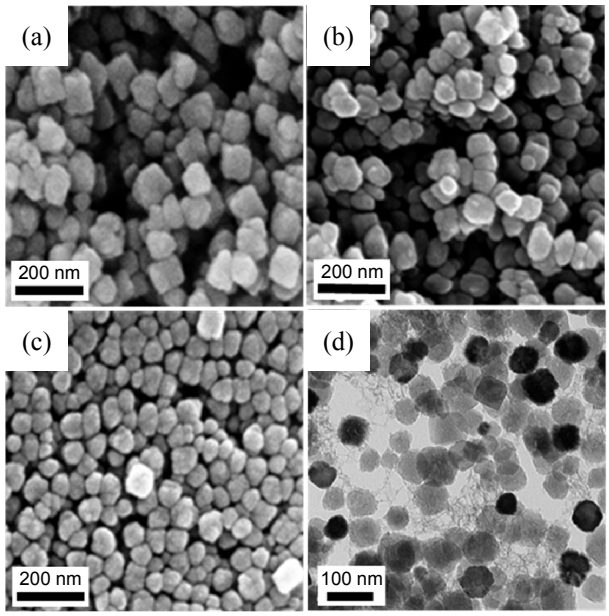

Figure 4. SEM images of the $Ba_xSr_{1-x}TiO_3$ nanoparticles in different Ba mol fractions [(a) $x = 0.25$, (b) $x = 0.5$, (c) $x = 0.75$], and TEM image of the as-prepared $Ba_{0.5}Sr_{0.5}TiO_3$ nanoparticles (d).

Differently from the typical sol-gel reactions, the concentration of titanium alkoxide in this synthetic approach was relatively high. Generally, overall inorganic sol-gel reaction of titanium alkoxide under moisture condition consists of the following hydrolysis (1) and condensation (2) steps.

$$Ti(OR)_4 + 4H_2O \rightarrow Ti(OH)_4 + 4ROH \quad (1)$$

$$Ti\text{-}OH + XO\text{-}Ti \rightarrow Ti\text{-}O\text{-}Ti + XOH \ (X = H \text{ or } R) \quad (2)$$

It is difficult to separate the hydrolysis (1) and condensation reactions (2) due to the high reactivity of titanium alkoxide.[23] Furthermore, at high concentration of titanium alkoxide, the sol-gel reaction is difficult to control: The as-prepared product will be severely aggregated, and the prepared titanate particles are not uniform in size. According to the report of Bradley *et al*., however, the presence of a strong base influences the condensation rate by the formation of TiO^- species.[24] Under the presence of $(CH_3)_4NOH$ (TMAH), the titanium alkoxide can be stabilized by forming a highly nucleophilic TiO^- ion.[20] As indicated in the equation (3), TiO^- can be stabilized in aqueous solution by forming the salt with $(CH_3)_4N^+$.

$$Ti\text{-}OH + (CH_3)_4NOH \rightarrow TiO^- + (CH_3)_4N^+ + H_2O \quad (3)$$

$$M(OOCCH_3)_2 \rightarrow M^{2+} (M = Sr \text{ or } Ba) + 2\ CH_3COO^- \quad (4)$$

$$M^{2+} + 2TiO^- \rightarrow Ti\text{-}O\text{-}M\text{-}O\text{-}Ti \quad (5)$$

As the Sr and Ba precursors, the acetate complexes were applied in the present work. These precursors are water-soluble and are expected to form metal cation in water, as shown in equation (4). The TiO^- is then favorably interacts with these metal cations (Sr^{2+}or Ba^{2+}) to form the polymeric inorganic chain structure, because of the high nucleophilicity of the TiO^- anionic species, as described in equation (5). Then the inorganic polymerization reactions proceed continuously to form sufficiently large particles with desired compositions and sizes. As a result, the nano-sized BST particles were successfully synthesized at relatively low temperature (< 100 °C) by the unique role TMAH in stabilizing the Ti-precursor.

Conclusion

$SrTiO_3$, $BaTiO_3$, and $Ba_xSr_{1-x}TiO_3$ (x = 0.25, 0.50 and 0.75) nanoparticles were synthesized by an inorganic sol-gel method at low temperature less than 100 °C. This low temperature procedure offers a simple and scalable synthetic route in preparing the highly crystallized BST nanoparticles. They were formed by the reactions with TiO^- ion stabilized by Me_4N^+ and M^{2+} ions (Sr^{2+} or Ba^{2+}). The synthesized BST nanoparticles were in a pure perovskite phase with average particle size of 70 - 80 nm, as characterized by XRD, SEM and TEM. The lattice parameter was linearly increased with increasing the Ba/Sr molar ratio from 0:1 to 1:0, suggesting that the complete solid solutions between $SrTiO_3$ and $BaTiO_3$ have been formed, regardless of compositions.

Acknowledgments. The authors gratefully acknowledge the financial support of Inha University (2010.03.01 - 2011.02.01).

References

1. Chandler, C. D.; Roger, C.; Smith, M. H. *J. Chem. Rev.* **1993**, *93*, 1205.
2. Pramanik, N. C.; Anisha, N.; Abraham, P. A.; Panicker, N. R. *J. Alloys Compd.* **2009**, *476*, 524.
3. Bhella, A. S.; Guo, R.; Roy, R. *Mater. Res. Innov.* **2000**, *4*, 3.
4. Dutta, P. K.; Asiaie, R.; Akbar, S. K.; Zhu, W. *Chem. Mater.* **1994**, *6*, 1542.
5. Wei, X.; Xu, G.; Ren, Z.; Wang, Y.; Shen, G.; Han, G. *J. Cryst. Growth* **2008**, *310*, 4132.
6. Ezhilvalavan, S.; Tseng, T. Y. *Mater. Chem. Phys.* **2000**, *65*, 227.
7. Carlson, C. M.; Rivkin, T. V.; Parilla, P. A.; Perkins, J. D.; Ginley, D. S.; Kozyrev, A. B.; Oshadchy, V. N.; Pavlov, A. S. *Appl. Phys. Lett.* **2000**, *76*, 1920.
8. Zimmermann, F.; Voigts, M.; Weil, C.; Jakoby, R.; Wang, P.; Menesklou, W.; Tiffée, E. I. *J. Eur. Ceram. Soc.* **2001**, *21*, 2019.
9. Ioachim, A.; Toacsan, M. I.; Banciu, M. G.; Nedelcu, L.; Vasiliu, F.; Alexandru, H. V.; Berbecaru, C.; Stoica, G. *Prog. Solid State Chem.* **2007**, *35*, 513.
10. Templeton, L. K.; Pask, J. A. *J. Am. Ceram. Soc.* **1959**, *42*, 212.
11. Mulder, B. J. *J. Am. Ceram. Soc. Bull.* **1970**, *49*, 990.
12. Kumazawa, H.; Annen, S.; Sada, E. *J. Mat. Sci* **1995**, *30*, 4740.
13. Phule, P. P.; Raghavan, S.; Risbud, S. H. *J. Am. Ceram. Soc.* **1987**, *70*, C108.
14. Li, Q.; Chen, D.; Jiao, X. *J. Alloys Compd.* **2003**, *358*, 76.
15. Brzozowski, E.; Castro, M. S. *J. Eur. Ceram. Soc.* **2000**, *20*, 2347.
16. Sharma, P. K.; Varadan, V. V.; Varadan, V. K. *Chem. Mater.* **2000**, *12*, 2590.
17. Roeder, R. K.; Slamovich, E. B. *J. Am. Ceram. Soc.* **1999**, *82*, 1665.
18. Gersten, B. L.; Lencka, M. M.; Riman, R. E. *J. Am. Ceram. Soc.* **2004**, *87*, 2025.
19. Xu, H.; Karadibhave, S.; Slamovich, E. B. *J. Am. Ceram. Soc.* **2007**, *90*, 2352.
20. Chen, C; Li, C.; Su, Q.; Peng, Q. *Mater. Res. Bull.* **2010**, *45*, 1762.
21. Viviani, M.; Buscaglia, M. T.; Testino, A.; Buscaglia, V.; Bowen, P.; Nanni, P. *J. Eur. Ceram. Soc.* **2003**, *23*, 1383.
22. Wada, S.; Tsurumi, T.; Chikamori, H.; Noma, T.; Suzuki, T. *J. Cryst. Growth* **2001**, *229*, 433.
23. Chemseddine, A.; Moritz, T. *Eur. J. Inorg. Chem.* **1999**, *2*, 235.
24. Bradley, D. C. *Adv. Chem. Series* **1959**, *23*, 10.